IRAQI BULLETIN OF GEOLOGY AND MINING (IBGM)\
IRAQ GEOLOGICAL SURVEY (GEOSURV-IRAQ)

*IBGM (**2025**, Vol 21; Issue 1)* *239-256*

PETROPHYSICAL ANALYSIS AND RESERVOIR EVALUATION OF THE SHIRANISH FORMATION USING WELL LOGS AND THIN SECTIONS IN A SELECTED WELL, NORTHERN IRAQ

Hussein S. Hussein[1*], Basoz J. Salih[2], Omer Th. Taher[2]

[1] Department of Petroleum Technology, Erbil Technology College, Erbil Polytechnic University, Erbil 44002, Kurdistan Region, Iraq,
[2] Department of Petroleum Geosciences, Soran University, Soran, Erbil 44002, Iraq.
***** *Corresponding author e-mail: hussein.suad@epu.edu.iq*

Type of the Paper (Article)
Received: 29/ 10/ 2024
Accepted: 12/ 02/ 2025
Available online: 27/ 06/ 2025

Abstract

Conventional well-logging methods are crucial for detecting petrophysical properties and are instrumental in reservoir characterization, particularly when subsurface rock samples are unavailable. In this study, log data and thin sections were employed to determine the petrophysical properties of the Late Campanian-Maastrichtian Shiranish Formation in the Kirkuk and Dukan area, Kurdistan Region, Iraq. Various approaches were integrated, including the Neutron-Density crossplot for lithology identification, Gamma-ray logs for determining shale volume, and sonic, density, and neutron logs for assessing porosity. The Shiranish Formation exhibits poor to fair porosity, with average values reaching 11.12% from the sonic log, 6.8% from the density log, and 8.4% from the neutron porosity log. Lithologies identified from the Neutron-Density crossplot indicate that the Shiranish Formation is predominantly composed of limestone and marly limestone. The determined shale volume within the examined interval reveals a high level of clay constituents in the lower part of the formation (2655 m-2693 m). The reservoir quality of the Shiranish Formation in the outcrop section is negligible, as evidenced by the thin section samples used in this study.

Keywords: Well logging; Petrophysical properties; Reservoir characterization; Shiranish Formation; Porosity.

1. Introduction

The Shiranish Formation, one of the most prevalent geological formations in Iraq, plays a critical role in understanding the country's geological history and its potential for hydrocarbon exploration. Filling the trough of the main synclines between the anticlines in the High Folded Zone, this formation exhibits significant variations in thickness and composition. The type locality of the Shiranish Formation is 227.5 meters thick, with the lower member comprising

ISSN 1811-4539, EISSN 3005-3714
https://doi.org/10.59150/ibgm2101a14
IBGM: http://ibgm-iq.org/
Academic Scientific Journals: www.iasj.net

marly limestone and marl, and the upper member consisting of bluish-grey, fine-crystalline limestone (Sissakian & Al-Jiburi, 2014). Spanning from the Late Campanian to the early Late Maastrichtian, the formation records a local transgressive-regressive cycle with marls and limestones as its primary constituents (Al-Dulaimi et al., 2023).

The Shiranish Formation is extensively distributed both in the subsurface and at outcrop in northern Iraq, contemporaneous with various other formations across the region. These include marls (such as the Jib'ab Marl), fore- or back-reef limestones (Bekhme and Aqra formations), and clastics (Tanjero Formation) (Al-Dulaimi et al., 2023). The lithostratigraphic relationships between these formations are intricate, often requiring biostratigraphic and sequence stratigraphic approaches for accurate correlation.

Several studies have focused on the reservoir characteristics, depositional environments, and lithological properties of Shiranish Formation(Aba Hassan, 1983; Abdallah & Al-Dulaimi, 2019; Abdula et al., 2018; Ahmed et al., 2017; Ahmed et al., 2023; Al Mutwali, 1996; Al-Banna, 2010; Al-Dulaimi et al., 2023; AL-Juboury et al., 2016; Awdal et al., 2013; Baban et al., 2020; Al-Qayim, 1993; El-Anbaawy & Sadek, 1979; Hassan, 2021; Kamil et al., 2021; Malak, 2015; Yonus et al., 2022). For instance, El-Anbaawy & Sadek (1979) showed that sediments of the Shiranish Formation have been deposited under shallow marine, moderately energetic, and weakly oxidizing alkaline conditions. Similarly, (Malak, 2015) described the depositional environment in Dukan as ranging from shallow-marine to upper-middle bathyal, based on sedimentological and biological evidence. This diversity in depositional environments is further supported by Abdula et al. (2018), who identified a deep basinal, pelagic environment for the formation in the Mergasur area. Baban et al. (2020) investigated the reservoir rock properties of the Late Cretaceous Shiranish Formation in the Taq Taq Oilfield, Kurdistan Region, Iraq. Their study, using well log and core data, identified key characteristics such as low porosity, less than 10%, and permeability generally under 10 mD, with fractures enhancing permeability in certain sections. They also distinguished three reservoir units based on variations in shale content, porosity, and permeability.

The formation's potential for industrial applications has also been explored. Additionally, (Awdal et al., 2013) used various geological and remote sensing data to analyze fracture characteristics, concluding that fracture intensity is primarily influenced by proximity to anticlines. There is a well-established relationship between fracture kinematics, fracture system geometry, and folding, as demonstrated in the works of Stearns & Friedman (1972) and Price (1966).

The primary objective of this research is to determine the petrophysical properties of the Shiranish Formation, including lithology, shale volume, and porosity, to evaluate its reservoir quality comprehensively.

2. Geological Setting

The studied well is located in the Khabbaz Oil Field (Figure 1), approximately 20 Km southwest of Kirkuk City and 23 Km southwest of the Baba Dome of the Kirkuk Oil Field. It lies parallel to the Kirkuk Oil Field and is situated tectonically within the Unstable Shelf in the Foot Hill Zone (Hamrin-Makhul Subzone) (Buday & Jassim, 1987). The field features an asymmetrical anticline with a northwest-southeast axis, characterized by a steeper northeast limb compared to the southwest limb. The structure measures approximately 18 km in length and 4 km in width(Al-Qayim et al., 2021).

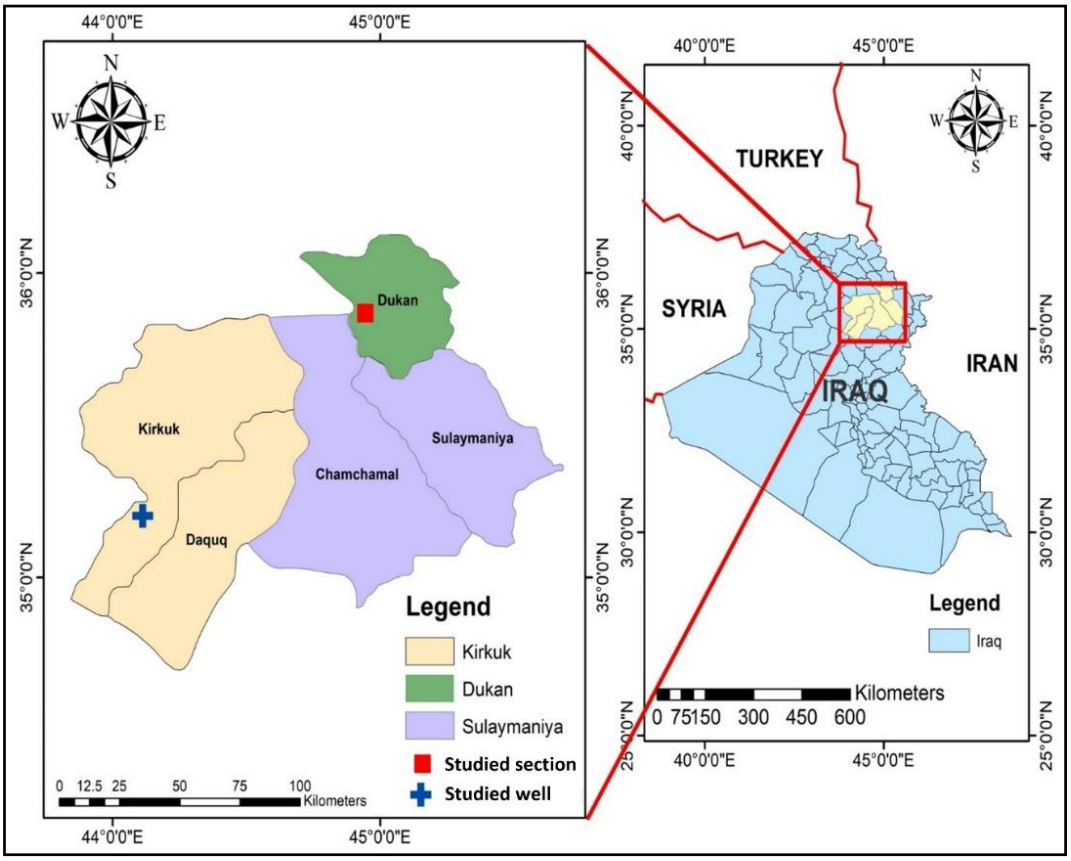

Figure 1. Location map of the studied well and the studied section.

The first seismic study of the Khabbaz region was conducted by the Iraqi Petroleum Company (IPC) in 1955, revealing a subsurface structure that descends toward the northwest (Baban & Hussein, 2016). Drilling commenced in August 1976 with well Kz-1, and the field was brought online in March 1994 by the Northern Oil Company (Baban & Hussein, 2016). Proven oil reserves in the Khabbaz Oil Field are estimated to exceed 0.5 billion barrels in its primary reservoir units, which include both Cretaceous and Tertiary reservoirs (Verma et al., 2004). Most of these wells have targeted the Kirkuk Group, although some wells have penetrated the underlying Shu'aiba Formation (Al-Qayim et al., 2021).

The Shiranish Formation, prominent near Dukan (Figure 1), is visible on the surface following the upper part of the Kometan Formation. In this area, the Shiranish Formation has a total thickness of 228 meters, though only 50 meters are exposed at the outcrop, with the remainder covered. This necessitates detailed measurement of rock properties such as porosity, permeability, and other petrophysical characteristics. The formation is widely distributed in Iraq, filling the troughs of main synclines between anticlines in the High Folded Zone. The thickness of the Shiranish Formation increases towards the center of the basin in northwestern Iraq and diminishes toward the basin's edges (Al-Dulaimi et al., 2023). This observation aligns with Sissakia's (2005) findings, which highlighted the significant thickness of Cretaceous formations in various regions of Iraq during the Cretaceous period. According to Henson (1940), as cited in Bellen et al. (1959), the thickness of the Shiranish Formation in the type section is approximately 225 m, with exposed thicknesses outside this region varying between 100 m and 400 m. In the Dukan region, the 228-meter-thick Shiranish Formation is exposed on the western limb of the Sarah anticline. It consists of thin beds of pelecypodal limestone at the top, soft bluish-gray marl rich in planktonic foraminifera, and dark gray marly limestone (Malak, 2015). The upper contact is conformable with the overlying Tanjero Formation, whereas the lower contact with the Turonian Kometan Formation is not conformable (Malak, 2015). The formation features six primary facies representing depositional settings from the middle shelf to the middle bathyal environment (Malak, 2015).

Maximum flooding surfaces (MFS) 165, 170, and 175, identified within three depositional sequences, show a good correlation with those in Iraq and other parts of the Arabian Plate (Aqrawi et al., 2010).

3. Methods

The methodology of this study is divided into two main groups based on the data obtained: field sampling and well log analysis. The primary goal was to determine the petrophysical properties of the Shiranish Formation through 120 meters of subsurface well logging data and the analysis of 9 thin sections collected at 44 m intervals along the formation's total thickness of 228 meters in the outcrop section.

For field sampling, nine rock samples were collected from the outcrop of the Shiranish Formation at various heights to capture a representative stratigraphic profile. The sampling points were at the following intervals from the lower part of the formation: 5m, 11m, 17m, 21m, 26m, 30m, 33m, 39m, and 44m, respectively, named sample 1 to sample 9. These samples were subjected to detailed lithological analysis to characterize the formation.

In the laboratory, thin sections of the rock samples were prepared and examined under a microscope to identify the amount of pore spaces in the samples was estimated using ImageJ software.

To supplement the rock sample analysis, well log data were utilized. The well logs provide a continuous record of the formation's properties, which helps in correlating and validating the field sample data. The available log data were digitized to facilitate detailed analysis. During digitization, five points were recorded for each meter to minimize measurement errors and enhance accuracy. The digitized data were then integrated into a well log database for further analysis.

Different types of well logs were employed to evaluate the Shiranish Formation due to their sensitivity to various formation components. These logs include the caliper log, which measures the diameter of the borehole and indicates changes in borehole size due to rock properties; the sonic log, which provides information on the acoustic properties of the formation and can be correlated to porosity and lithology; the gamma-ray log, which measures natural radioactivity to differentiate between shale and non-shale formations; the neutron porosity log, which estimates the porosity of the formation by measuring hydrogen content, typically in the form of water or hydrocarbons; and the bulk density log, which measures the density of the formation and helps in identifying different rock types and estimating porosity.

Several software were utilized to process and analyze the data collected. GIS software was used to map the study area and manage geographic and spatial data. Get Data Graph Digitizer was employed to digitize curves from the well logs. Grapher 12 was used to create and analyze curve logs, transforming complex data into visual tools such as maps and graphs.

4. Results and Discussion

4.1. Lithology Identification and Shale Content

4.1.1. Lithology Determination from Porosity Logs

In the oil industry, logging services have devised numerous techniques to ascertain the lithology of drilled rock sequences using log data. These are considered indirect methods of lithology determination since they do not involve direct examination of rock samples (Priisholm & Michelsen, 1979).

Accurate lithology identification is crucial for evaluating a reservoir. It cannot be inferred from a single tool measurement alone; instead, it requires the combined data from multiple logs to accurately determine the formation's lithology (Hussein, 2023; Hussein et al., 2024).

4.1.2. Neutron-density crossplot

A crossplot combines multiple log measurements, specifically neutron and density logs, to create an N-D (Neutron-Density) crossplot. This plot features three diagonal lines that represent different lithology types: dolomite, calcite (limestone), and quartz matrix with water-filled porosity.

The blue dots on the crossplot represent subsurface measurements of bulk density and neutron porosity, offering insights into the lithology of the formation (Figure 2). The majority of the data points align closely with the "Calcite (limestone)" trend, suggesting that limestone is the predominant lithology, which aligns with standard interpretations of carbonate rocks in similar density-porosity crossplot (Schlumberger, 2013). However, some points trend toward the "Quartz Sandstone" line, which may indicate the presence of siliciclastic input into the carbonate system. Such trends are often associated with mixed carbonate-siliciclastic systems, where marl or marly limestone, a mixture of carbonate and siliciclastic material, can form in depositional environments influenced by siliciclastic sediment influx (Tucker & Wright, 2009). Marl or marly limestone typically forms where silt and clay are introduced into carbonate settings, a common occurrence in transitional or shallow marine environments. This interpretation, based on data plotted along the sandstone line or between limestone and sandstone to marl or marly limestone, aligns with the rock descriptions of the Shiranish Formation in the studied section. Additionally, some points near the "Dolomite" trend suggest localized dolomitization, consistent with diagenetic processes that replace calcite with dolomite under specific geochemical conditions (Moore, 2001).

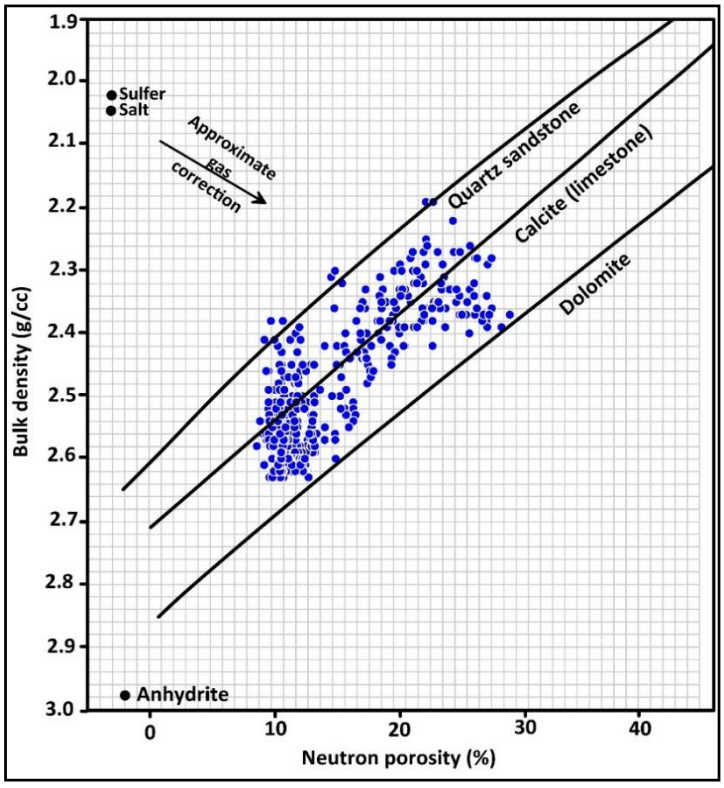

Figure 2. Illustrates the relationship between bulk density (ρb), corrected apparent limestone neutron porosity, and lithology lines for common rock types. Gas correction refers to adjustments made to account for the effects of gas presence on density and neutron porosity readings, ensuring accurate interpretation (Schlumberger, 2013).

The lithological column in Figure 3a represents various rock types with depth, as estimated from the well-log measurements, showing a predominance of limestone (blue) throughout most

of the interval, particularly in the upper unit. Dolomite (orange) appears in smaller intervals, while dolomitic limestone (red) alternates with other lithologies, especially between depths of 2625 – 2645 meters. A comparison with Figure 2, dolomitic limestone, represents data plotted between the dolomite and limestone lines (Bowler, 1981). Marl (yellow) is sparsely distributed and plotted within the sandstone region, while marly limestone (green) occurs more frequently and is positioned between limestone and sandstone intervals.

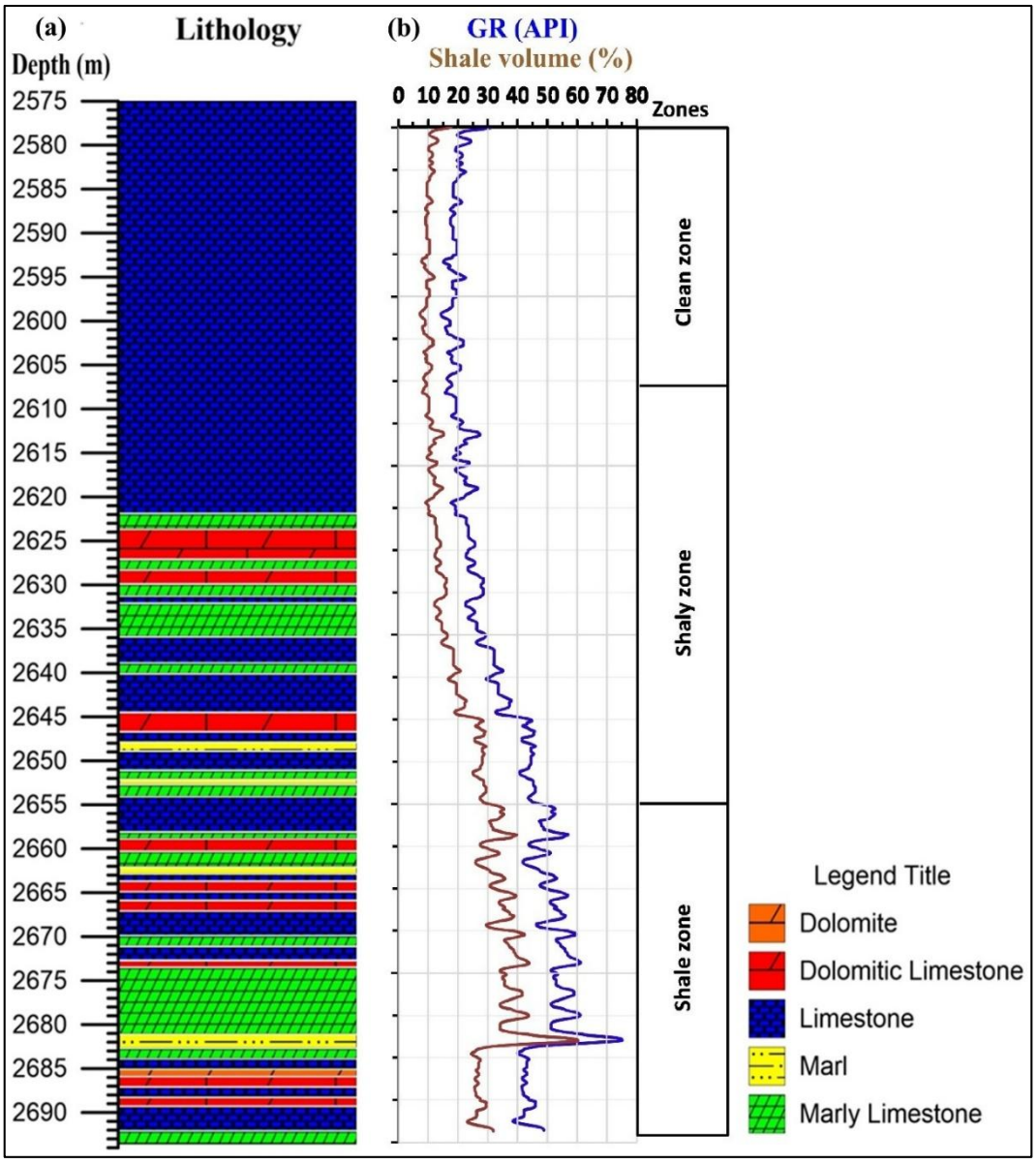

Figure 3. **a**) Lithological column derived from log data for estimating the lithology. **b**) Gamma-ray log, shale volume curve, and shale zonation categorized by the percentage of shale volume in the Shiranish Formation (Ghorab et al., 2008).

4.1.3. Gamma-ray log

Radiation emanating from uranium, thorium, potassium, and their decay products collectively contributes to the response observed in the standard gamma ray log (Asquith et al., 2004).

Examining the sources of natural gamma radiation provides valuable insights into the lithology and composition of the formation.

In this study, a gamma-ray (GR) curve (Figure 3b) was utilized to identify lithology and estimate shale volume. Shale, which typically contains higher concentrations of radioactive elements, exhibits elevated gamma-ray readings (Asquith et al., 2004).

The conventional gamma-ray log assumes that shale is the predominant source of radioactive minerals when quantifying shale volume within the formation (Asquith et al., 2004).

Gamma-ray log data were employed to calculate the shale volume in the reservoir rocks. This calculation is crucial as the shale volume threshold is often employed to differentiate between reservoir and non-reservoir rocks. Initially, the IGR (gamma ray index) is derived from the gamma-ray log using Equation 1.

$$IGR = (GR_{log} - GR_{min}) / (GR_{max} - GR_{min}) \quad (1)$$

where GR_{log} = the gamma-ray log reading, GR_{min} = the minimum gamma-ray log reading, and GR_{max} = the maximum gamma-ray log reading.

Based on the age of the studied formation, Larionov's equation for the older rocks is used to determine shale volume (Asquith et al., 2004; Equation 2).

$$Vsh = 0.33 (2^{2*IGR} - 1) \quad (2)$$

Where Vsh: Shale volume and IGR: Gamma-ray index.

Table 1 presents the classification of shale zonation, utilizing the percentage of shale volume to classify shale deposits based on the standard proposed by Ghorab et al. (2008). This method distinguishes various shale zones based on the shale contents in the formation. In our investigation of the Shiranish Formation, the shale volume was estimated from gamma-ray data across various intervals (Figure 3b). The studied formation is divided into three distinct zones: 2575 to 2610 meters as a clean zone, 2611 to 2655 meters as a shaly zone, and 2655 to 2693 meters as the interval with the highest shale volume (Figure 3b).

Table 1. Shale zonation is categorized by the percentage of shale volume according to categories suggested by Ghorab et al. (2008).

Shale volume (%)	Zones
<10	Clean zone
10 – 35	Shaly zone
>35	Shale zone

4.1.4. Caliper log

In this study, the caliper log serves to identify both mud cake formation and permeable zones. Analysis of the caliper readings reveals that the hole diameter is smaller than the bit size, indicating a mud cake buildup of 0.2 inches thick within the limestone unit spanning 2575 to 2635 meters, signifying a permeable zone (Figure 4). Conversely, beyond 2635 to 2658 meters in limestone, marly limestone, and marl units, the hole diameter exceeds the bit size, possibly due to erosion from circulating borehole mud or interference from the turning drill pipe, resulting in sections that appear "washed out" (Figure 4). Furthermore, there is a minor enlargement in the borehole wall between 2661 and 2664 meters, and a more pronounced enlargement from 2670 to 2693 meters (Figure 4).

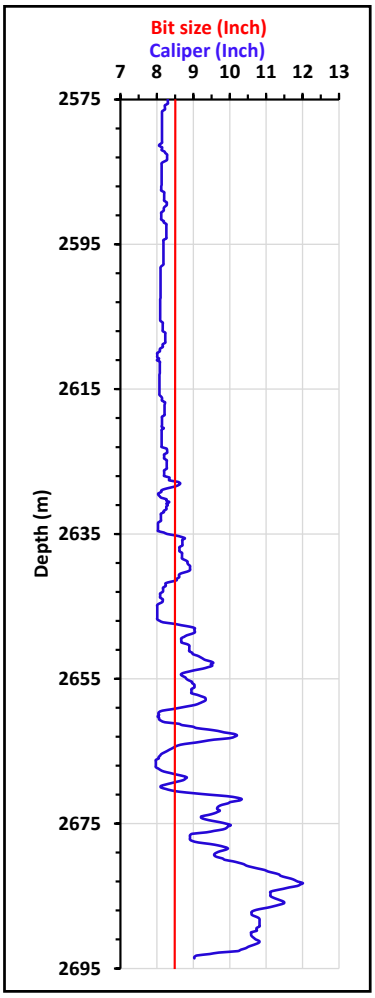

Figure 4. Caliper log and bit size data for the Shiranish Formation, showing borehole diameter variations and formation stability.

4.2. Porosity Estimation and Porosity Units

Shale presence increases the calculated porosity values across all porosity logs (Baban & Hussein, 2016), requiring corrections that primarily depend on shale volume. Corrected

porosity values are presented, with Figures 5 and 6 illustrating the corrected porosities for the studied formations. Among the tools, the neutron log is most affected by shale, likely due to the free and bound water in shale, which exhibits a high hydrogen index (Asquith et al., 2004), leading to overestimated porosity values. In contrast, density and sonic logs are less affected. Consequently, shale porosity must be subtracted from the total porosity to determine the effective reservoir porosity. The identification of shale distribution types is crucial for understanding its impact on reservoir quality. Shale distribution significantly influences reservoir properties, and there are three primary types: structural, laminated, and dispersed. In the case of the Shiranish Formation, the shale is characterized by a dispersed distribution type (Baban et al., 2020).

4.2.1. Sonic porosity

When pores contain hydrocarbon liquids or gases, the speed of sound decreases, resulting in longer transit times through the formation. Conversely, in the absence of pore spaces and with a solid medium, the speed of sound increases, leading to shorter transit times (Asquith et al., 2004). Equations 3 and 4 are used to calculate uncorrected sonic porosity and corrected porosity, respectively.

$$\Phi_{sonic} = (\Delta t_{log} - \Delta t_{ma}) / (\Delta t_{fl} - \Delta t_{ma}) \quad (3)$$

$$\Phi_{scorr} = (\Delta t_{log} - \Delta t_{ma}) / (\Delta t_{fl} - \Delta t_{ma}) - V_{sh} (\Delta t_{sh} - \Delta t_{ma}) / (\Delta t_{fl} - \Delta t_{ma}) \quad (4)$$

Where Φ_{sonic}: Porosity from sonic log (uncorrected), Φ_{scorr}: Corrected sonic porosity, Δt_{log}: Interval transit time of the formation (μsec/ft), Δt_{ma}: Interval transit time of the matrix (μsec/ft), $\Delta t_{fl:}$ Interval transit time of the fluid (μsec/ft), Δt_{sh}: Interval transit time of shale (μsec/ft), and V_{sh}: Volume of shale.

Figure 5 consists of two graphs illustrating the variation of sonic transit time and sonic porosity with depth for the studied formation. Graph A shows the interval transit time (in microseconds per foot) plotted against depth, highlighting variations in the acoustic properties of the formation. Graph B presents the corrected and uncorrected sonic porosity (%) for the same depth interval, with blue representing the corrected porosity and red indicating the uncorrected porosity. The data reveal that shale corrections significantly reduce porosity values in zones with higher shale content, emphasizing the necessity of shale correction for accurate reservoir characterization.

Porosity from the sonic log is divided into three intervals, with the average and maximum values detailed as follows:

- For the interval 2575 – 2620 meters, the average porosity is 10.7%, and the maximum is 12.9%.
- In the interval 2621 – 2661 meters, the average porosity decreases to 9.4%, with the maximum reaching 11.4%.
- Within the interval 2662 – 2693 meters, the average porosity is 13.9%, and the maximum is 21.6%.

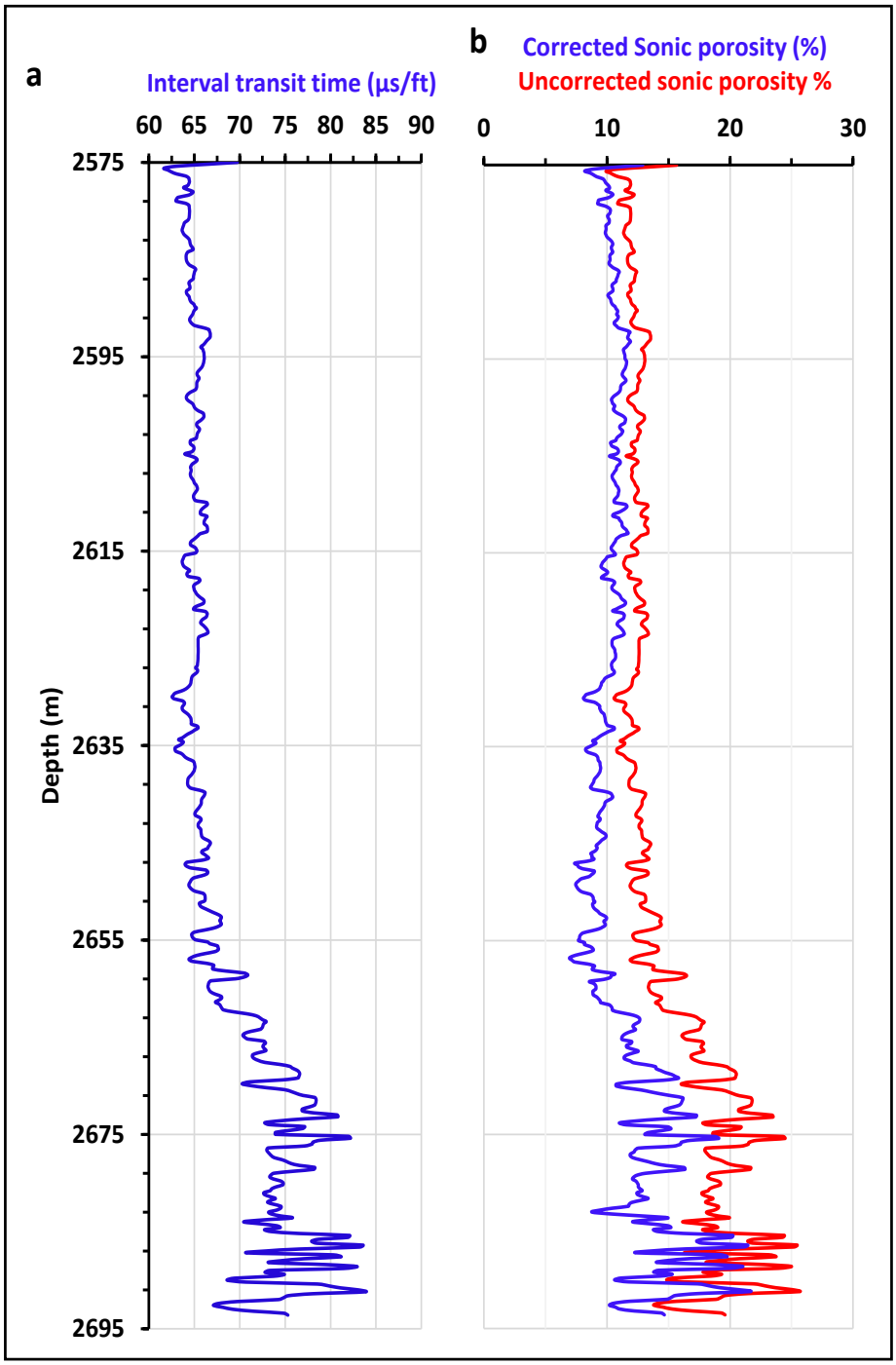

Figure 5. a) Interval transit time (µs/ft) and (b) sonic porosity of the studied formation, including both corrected sonic porosity (%) and uncorrected sonic porosity (%), highlighting their variation with depth.

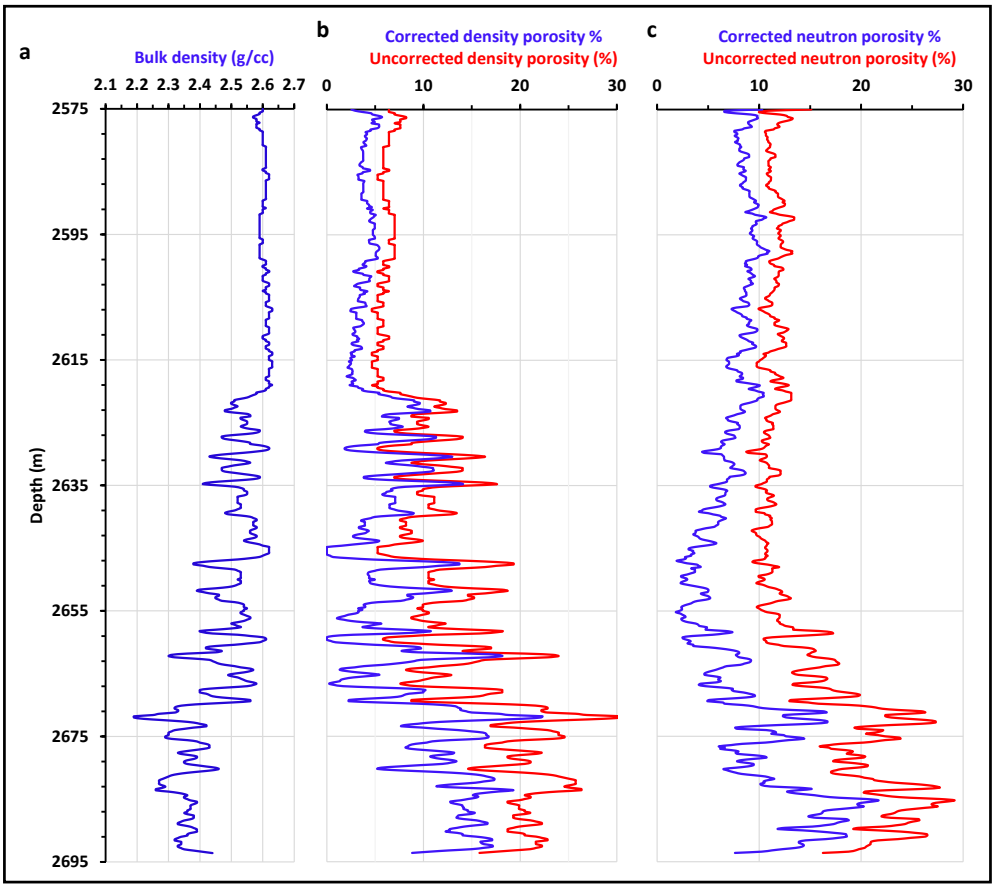

Figure 6. Variations of Shiranish Formation in (a) bulk density (g/cc), (b) uncorrected density porosity and corrected density porosity (%), and (c) uncorrected neutron porosity and corrected neutron porosity (%), providing a comparative analysis of these parameters across the measured depth intervals.

4.2.2. Density and neutron porosity

Figure 6 demonstrates three graphs that present bulk density and porosity variations with depth. Graph A displays bulk density (g/cc) plotted against depth, with fluctuations indicating changes in lithology and formation compaction. Graph B compares the corrected (blue) and uncorrected (red) density porosity (%), showing the impact of shale content corrections. Graph C illustrates the corrected (blue) and uncorrected (red) neutron porosity (%), where neutron porosity is notably higher in shale-rich zones due to the high hydrogen index of bound water in shale. The overall trends highlight the necessity of shale corrections to obtain more accurate porosity values, emphasizing the variability of reservoir properties within the studied interval. Equations 5, 6, and 7 are used to calculate uncorrected density porosity, corrected density porosity, and corrected neutron porosity, respectively.

$$\Phi D = (\rho_{ma} - \rho_b) / (\rho_{ma} - \rho_{fl}) \quad (5)$$

$$\Phi_{Dcorr} = (\rho_{ma} - \rho b) / (\rho_{ma} - \rho_{fl}) - V_{sh}(\rho_{ma} - \rho_{sh}) / (\rho_{ma} - \rho_{fl}) \quad (6)$$

Where Φ_D = Porosity from density log (uncorrected), Φ_{Dcorr} = Corrected density porosity, ρ_{ma}: Matrix density, ρ_b: Bulk density, ρ_{sh}: Shale bulk density, ρ_{fl}: Fluid density, and V_{sh}: Volume of shale.

Porosity from the density log is divided into three intervals, with the average and maximum values detailed as follows:

- For the interval 2575 – 2620 meters, the average porosity is 3.4%, and the maximum is 6.8%.
- In the interval 2621 – 2661 meters, the average porosity increases to 6.1%, with the maximum reaching 14%.
- Within the interval 2662 – 2693 meters, the average porosity is 11.8%, and the maximum is 22.3%.

$$\Phi_{Ncorr} = \Phi_N - V_{sh} \times \Phi_{Nsh} \quad (7)$$

Where Φ_{Ncorr}: Corrected Neutron porosity, Φ_N: Neutron porosity (uncorrected), and Φ_{Nsh}: Neutron porosity of shale.

The neutron porosity can also be subdivided into three zones, similar to density and sonic porosity. The average neutron porosity values for the three intervals or zones are 8.9%, 5.4%, and 11.4%, respectively, while the maximum neutron porosity values are 10%, 6.3%, and 21.7%, respectively.

4.3. Porosity Units

Based on porosity measurements and log analysis of the Shiranish Formation, it has been divided into three porosity units (Unit-1, Unit-2, and Unit-3) from top to bottom, as illustrated in Figure 7. Table 2 summarizes the average porosity values derived from sonic, density, and neutron logs across these three units.

Unit 1: This unit shows 10.7% porosity from Sonic, 3.4% from Density, and 8.9% from neutron. While the porosity values calculated from the density are the lowest, sonic and neutron values indicate relatively higher porosity compared to unit 2.

Unit 2: This unit displays a slight increase in density porosity compared to unit 1. The sonic porosity is 9.4%, density shows 6.1%, and neutron readings show 5.4%, with more consistency between density and neutron readings.

Unit 3: The highest porosity values are recorded in this unit, with 13.9% from sonic, 11.8% from density, and 11.4% from neutron. All methods provide closely aligned porosity readings, indicating higher and more consistent porosity in this unit.

Table 2 shows that porosity increases progressively from unit 1 to unit 3. Moreover, the density method consistently shows slightly lower porosity than the sonic and neutron porosity in Unit-1 but aligns more closely in Unit-2 and Unit 3. The lower average porosity in unit 1 for density porosity is due to the presence of mud cake within the interval (2575 – 2621 m), as indicated in Table 2.

Table 2. Average porosity values derived from sonic, density, and neutron logs of the studied formation.

Units (m)	Average porosity (%)		
	Sonic	**Density**	**Neutron**
unit 1	10.7	3.4	8.9
unit 2	9.4	6.1	5.4
unit 3	13.9	11.8	11.4

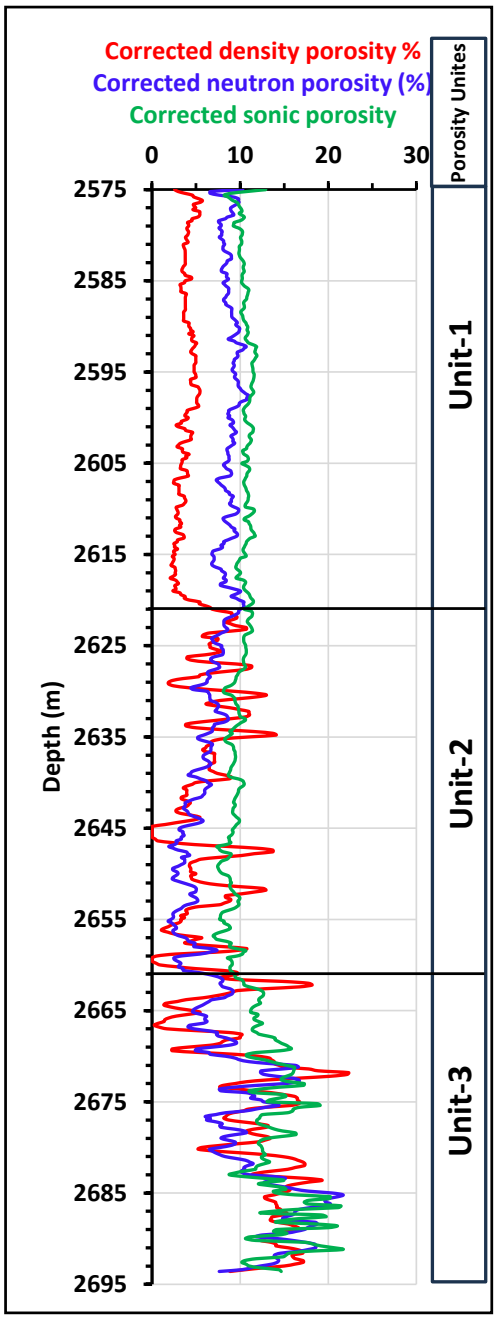

Figure 7. Three porosity units, unit 1 to unit 3, are distinguished from the results of density, sonic, and neutron logs of the Shiranish Formation. See the text for more explanation.

Based on our findings (Table 2) and the classification by North (1985) (Table 3), the porosity in unit 1 is assessed as poor to fair. Unit 2 generally exhibits poor porosity levels across all porosity logs. In contrast, unit 3 demonstrates fair porosity values across all available porosity logs.

Table 3. Qualitative characterization of porosity as suggested by North (1985).

Percentage Porosity (%)	Qualitative Description
0 – 5	Negligible
5 – 10	Poor
10 – 15	Fair
15 – 20	Good
20 – 30	Very Good
> 30	Excellent

4.4. Porosity from thin sections

Nine thin sections, impregnated with blue resin, were prepared from the outcrop section of the Shiranish Formation (Figure 8, images 1 – 9). These images display the pore structure of the studied formation under the microscope at a magnification of x2.5. The blue resin technique was employed for porosity measurement. Table 4 displays the quantitative average porosity among all nine samples of the studied formation, which is 4.2%. This indicates that the average porosity of the Shiranish Formation is very low, making it negligible in terms of total qualitative porosity. The low porosity might result from the outcrop of the Shiranish Formation being minimally fractured. Additionally, there could have been errors during the preparation of the thin section samples, where some very tiny grains might not have been covered with blue resin, making them invisible under the microscope. As a key petrophysical characteristic of a reservoir is to have high porosity to trap hydrocarbons effectively, the Shiranish Formation, based on our results, cannot be considered a good reservoir due to its very low porosity, which would not be conducive to accumulating hydrocarbons.

Table 4. Porosity classification is categorized by the percentage of pore volume in thin sections.

Sample No.	Average Porosity (%)	Qualitative Description
1	8.46	Fair
2	0.02	Negligible
3	16.01	Good
4	7.2	Poor
5	0.02	Negligible
6	1.35	Negligible
7	0.59	Negligible
8	3.03	Negligible
9	1.86	Negligible

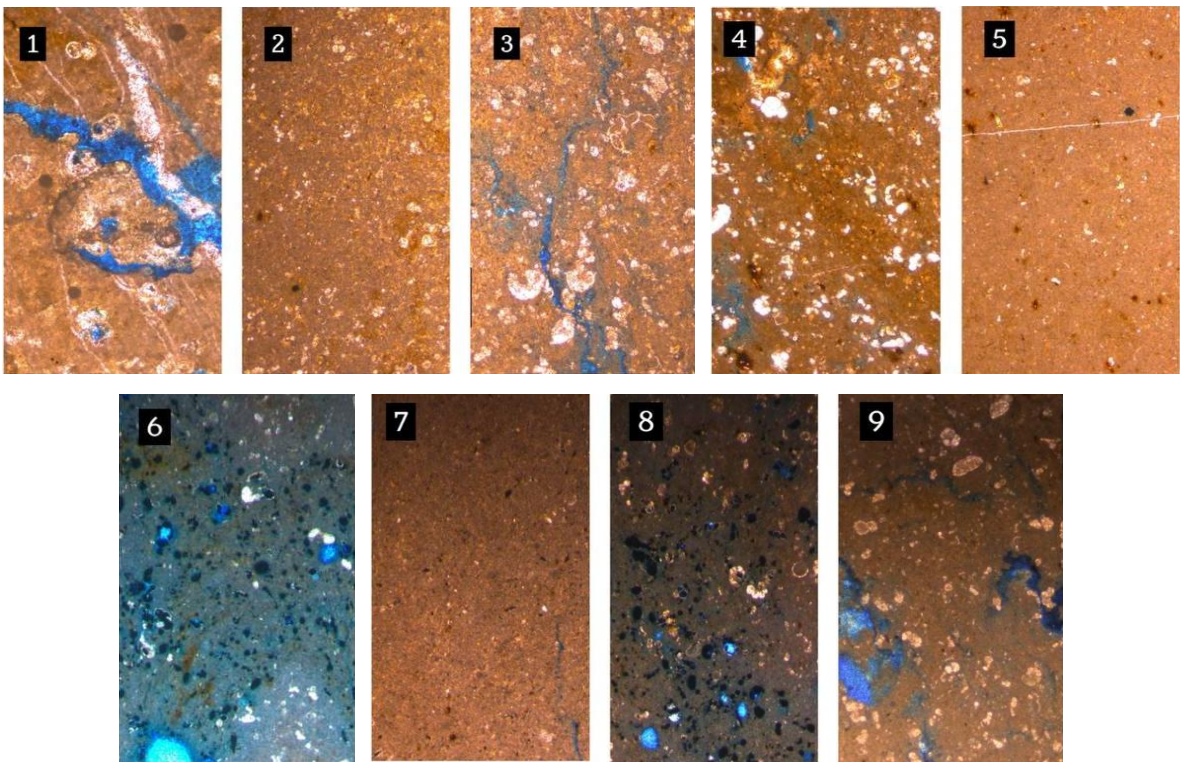

Figure 8. Thin sections of the Shiranish Formation are impregnated with blue-dyed resin, highlighting pore spaces (blue). The images show variable porosity: (1, 3, 6, 9) high porosity; (4, 8) moderate porosity; (2, 5, 7) low to negligible porosity.

5. Conclusions

The formation is predominantly composed of limestone, with notable occurrences of marly limestone, marl, and dolomitic limestone, reflecting diverse depositional environments. Porosity increases progressively from unit 1 to unit 3, with unit 3 exhibiting the highest porosity values across all log types. This variability underscores the influence of lithology and diagenetic processes on reservoir quality. Gamma-ray logs identified significant shale content, particularly in the lower part. Moreover, thin section analysis confirmed very low porosity (averaging 4.2%) in outcrop samples, suggesting limited reservoir potential in these sections due to minimal microfracturing and possible sampling limitations. Finally, despite localized zones of enhanced porosity, the overall characteristics of the Shiranish Formation indicate poor to fair reservoir quality, limiting its suitability for hydrocarbon accumulation without significant secondary enhancements.

References

Aba Hassan, A. (1983). Petrography and geochemical study for selected sections of the formation of Shiranish in northern Iraq. *Unpublished M.Sc. Thesis, University of Baghdad, Faculty of Science.*

Abdallah, F. T., & Al-Dulaimi, S. I. (2019). Biostratigraphy of the Upper Cretaceous for selected sections in northern Iraq. *Iraqi Journal of Science*, *60*(3), 545–553. https://doi.org/10.24996/ijs.2019.60.3.14

Abdula, R. A., Balaky, S., Miran, A., Muhamad, C., Khailany, R., & Muhammad, M. (2018). Sedimentology of the Shiranish Formation in the Mergasur area, Iraqi Kurdistan. *Bulletin of the Geological Society of Malaysia*, *65*(1), 37–43. https://doi.org/10.7186/bgsm65201804

Ahmed, M. R., Al-Rashidi, M. A., & Alkhafaji, M. W. (2017). The Sedimentology and Facies Analysis of the Cretaceous Oceanic Red Beds (CORBs) in the Shiranish Formation, Northern of Iraq. *IRAQI JOURNAL OF SCIENCE*, *58*(3A). https://doi.org/10.24996/ijs.2017.58.3a.6

Ahmed, M. R. M., Al-Rashidi, M. A., & Alkhafaji, M. W. (2023). Hydrocarbon Potential and Depositional Environment of the Shiranish Formation in Northern Iraq. *Iraqi Geological Journal*, *56*(2), 237–246. https://doi.org/10.46717/igj.56.2A.18ms-2023-7-27

Al Mutwali, M. (1996). Planktonic foraminiferal biostratigraphy of the Shiranish Formation, Khashab well (No. 1), Hemren area, northeastern Iraq. *Rafidain Journal of Science*, *7*, 129–136.

Al-Banna, N. Y. (2010). Sequence stratigraphy of the Late Campanian - Early Maastrichtian Shiranish Formation, Jabal Sinjar, northwestern Iraq. In *GeoArabia* (Vol. 15, Issue 1, pp. 31–44). Gulf Petrolink. https://doi.org/10.2113/geoarabia150131

Al-Dulaimi, A. M., Al-Haj, M. A., Asaad, I. S., Omar, N., & Zanoni, G. (2023). Depositional Setting of the Shiranish Formation (Campanian-Maastrichtian) in Selected Sections from Northern Iraq. *Iraqi Geological Journal*, *56*(1F), 207–225. https://doi.org/10.46717/igj.56.1F.14ms-2023-6-22

Al-Juboury, F., A . Al-Juboury, W., & M.AL-Taraf, A.-S. (2016). Microfacies and depositional environment of Shiranish Formation in Ain Zalah and Butmah Oil fields north west Iraq. *Kirkuk University Journal-Scientific Studies*, *11*(2), 438–463. https://doi.org/10.32894/kujss.2016.124645

Al-Qayim, B. (1993). Bioturbated Rhythmite of the Shiranish Formation, Type Locality, NW Iraq. *Iraqi Geological Journal*, *25*(1), 185–194.

Al-Qayim, B., Qader, F., & Albeyati, F. M. O. (2021). Evaluation of reservoir fluids mobility, Mauddud Reservoir (Albian), Khabbaz oil field, Kirkuk area, NE Iraq. *Iraqi Geological Journal*, *54*(2), 42–54. https://doi.org/10.46717/igj.54.2B.4Ms-2021-08-24

Aqrawi, A., Jeremy Goff, Andrew Horbury, & Fadhil Sadooni. (2010). *The Petroleum Geology of Iraq* (Vol. 424). Scientific Press.

Asquith, G., Krygowski, D., Henderson, S., & Hurley, N. (2004). *Basic well log analysis*. American Association of Petroleum Geologists. https://doi.org/10.1306/Mth16823

Awdal, A. H., Braathen, A., Wennberg, O. P., & Sherwani, G. H. (2013). The characteristics of fracture networks in the Shiranish Formation of the Bina Bawi Anticline; comparison with the Taq Taq Field, Zagros, Kurdistan, NE Iraq. *Petroleum Geoscience*, *19*(2), 139–155. https://doi.org/10.1144/petgeo2012-036

Baban, D. H., Qadir, F. M., & Mohammed, A. R. (2020). Reservoir Rock Properties of the Upper Cretaceous Shiranish Formation in Taq Taq Oilfield, Iraqi Kurdistan Region. In *JZS-A* (Vol. 22, Issue 1). http://jzs.univsul.edu.iq

Baban, D., & Hussein, H. (2016). Characterization of the Tertiary reservoir in Khabbaz Oil Field, Kirkuk area, Northern Iraq. *Arabian Journal of Geosciences*, *9*(3), 237. https://doi.org/10.1007/s12517-015-2272-y

Bellen, R. C., Dunnington, H. V., Wetzel, R., & Morton, D. (1959). Lexique Stratigraphique International, Asie, Iraq . *International Geological Congress*, *3*.

Bowler, J. (1981). THE LITHO-DENSITY* LOG. *The APPEA Journal*, *21*(1), 200. https://doi.org/10.1071/AJ80022

Buday, T., & Jassim, S. (1987). *The regional geology of Iraq* (Vol. 2). GEOSURV.

El-Anbaawy, M. I. H., & Sadek, A. (1979). Paleoecology of the Shiranish Formation (Maestrichtian) in northern Iraq by means of microfacies analysis and clay mineral investigation. *Palaeogeography, Palaeoclimatology, Palaeoecology*, *26*, 173–180. https://doi.org/10.1016/0031-0182(79)90148-2

Ghorab, M., Ramadan, M., & Nouh, A. (2008). The relation between the shale origin (source or non-source) and its type for Abu Roash Formation at Wadi El-Natrun area, south of Western Desert, Egypt. *Australian Journal of Basic and Applied Sciences*, *2*(3), 360–371.

Hassan, Y. (2021). *Biostratigraphy of foraminiferal and depositional environment of Shiranish Formation in Sara Anticline in Dokan Area/Sulaymani, Northeastern Iraq*. University of Mosul.

Henson, F. (1940). *Shiranish Formation (Cretaceous). Unpublished report. In van Bellen, R. C., Dunnington, H. V., Wetzel, R., & Morton, D. M. (1959). Lexique stratigraphique international, Asie*.

Hussein, H. S. (2023). Electrofacies Analysis using a Geostatistical Approach, Northern Iraq Case Study. *Polytechnic Journal*, *13*(2), 58–67. https://doi.org/10.59341/2707-7799.1723

Hussein, H. S., Mansurbeg, H., & Bábek, O. (2024). A new approach to predict carbonate lithology from well logs: A case study of the Kometan formation in northern Iraq. *Heliyon*, *10*(3), e25262. https://doi.org/10.1016/j.heliyon.2024.e25262

Kamil, A. I., Al-Dulaimi, S., & Karim, K. H. (2021). Ammonites and Foraminifera of Shiranish Formation (Late Campanian-Maastrichtian) from Sulaimaniya and Erbil Governorates, Northern Iraq. *Iraqi Journal of Science*, *62*(12), 4712–4746. https://doi.org/10.24996/ijs.2021.62.12.12

Malak, Z. A. (2015). Sequence stratigraphy of Shiranish Formation in Dokan area, Northern Iraq. *Arabian Journal of Geosciences*, *8*(11), 9489–9499. https://doi.org/10.1007/s12517-015-1885-5

Moore, C. H. (2001). Diagenetic environments of porosity modification and tools for their recognition in the geologic record. In Carbonate reservoirs: Porosity evolution and diagenesis in a sequence stratigraphic framework. *Developments in Sedimentology*, *55*, 61–88.

North, F. K. (1985). *Petroleum geology*.

Price, N. (1966). *Fault and Joint Development in Brittle and Semi-Brittle Rock*. Elsevier. https://doi.org/10.1016/C2013-0-05410-2

Priisholm, S., & Michelsen, O. (1979). THE USE OF POROSITY LOGS IN LITHOLOGY DETERMINATION, LITHOSTRATIGRAPHY AND BASIN ANALYSIS. In *Geomathematical and Petrophysical Studies in Sedimentology* (pp. 71–79). Elsevier. https://doi.org/10.1016/B978-0-08-023832-6.50013-9

Schlumberger. (2013). *Log interpretation charts* (2013th ed.). https://www.spec2000.net/downloads/SLB%20Chartbook%202013.pdf

Sissakian, V. K. (2005). THE STRATIGRAPHY OF THE EXPOSED CRETACEOUS ROCKS IN IRAQ, AS DEDUCED FROM THE RESULTS OF THE REGIONAL AND DETAILED GEOLOGICAL SURVEYS (GEOSURV 1971-1996). In *Iraqi Bulletin of Geology and Mining* (Vol. 1, Issue 1).

Sissakian, V. K., & Al-Jiburi, B. S. M. (2014). STRATIGRAPHY OF THE HIGH FOLDED ZONE. In *Iraqi Bull. Geol. Min., Special Issue* (Issue 6).

Stearns, D. W., & Friedman, M. (1972). Reservoirs in fractured rock. *Geologic Exploration Methods*, 82–106.

Tucker, M. E., & Wright, V. P. (2009). *Carbonate sedimentology* (second). John Wiley & Sons.

Verma, M. K., Ahlbrandt, T. S., & Al-Gailani, M. (2004). *Petroleum reserves and undiscovered resources in the total petroleum systems of Iraq: reserve growth and production implications*. http://pubs.geoscienceworld.org/gpl/geoarabia/article-pdf/9/3/51/5441684/verma.pdf

Yonus, W. A., Fadhil, D. T., & Theyab, M. A. (2022). The Use of Borehole Logs to Study the Reservoir Properties of Shiranish Formation in Qayarah Field in Northern Iraq. *AIP Conference Proceedings*, *2660*. https://doi.org/10.1063/5.0109106

About the author

Hussein S. Hussein is a geologist and well-logging expert with a Ph.D. in Geology, specializing in reservoir characterization. He has extensive experience in petroleum geology, formation evaluation, and fracture analysis, with a focus on carbonate reservoirs in the Kurdistan Region of Iraq. Dr. Hussein has authored multiple peer-reviewed publications and is actively involved in research on stylolite, and the application of neural networks and multiple linear regression in log data interpretation. He also serves as a lecturer, teaching well logging, reservoir characterization, and petroleum geology.

e-mail: hussein.suad@epu.edu.iq

Basoz J. Salih and **Omer Th. Taher** are researchers who hold Bachelor's degrees in Petroleum Geosciences. Their academic background provides a solid foundation in geological and petrophysical concepts related to hydrocarbon exploration.